Science Advances
AAAS

Supplementary Materials for

Mice with humanized livers reveal the role of hepatocyte clocks in rhythmic behavior

Anne-Sophie Delbès *et al.*

Corresponding author: Serge Luquet, serge.luquet@u-paris.fr, Frédéric Gachon, f.gachon@uq.edu.au

Sci. Adv. **9**, eadf2982 (2023)
DOI: 10.1126/sciadv.adf2982

The PDF file includes:

Other Supplementary Material for this manuscript includes the following:

Fig. S1

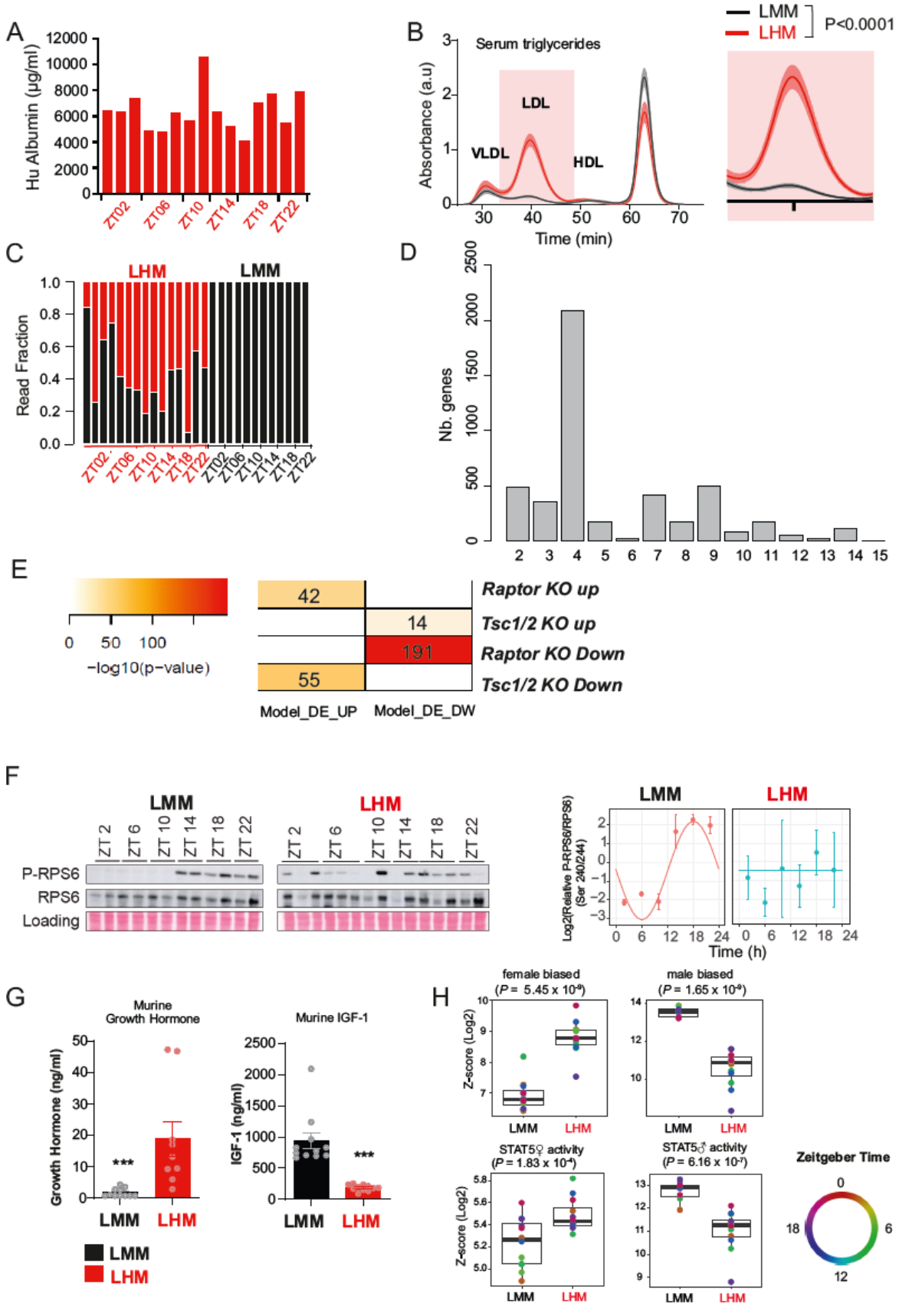

Fig.S1. Characterization of the humanized mouse model and its impact on liver gene expression

A) Plasma level for human albumin in LHM mice 2 months after primary hepatocyte engraftment and before sacrifice at different ZT times. Human albumin is non-detectable in LMM.

B) Plasma triglyceride (TG) Lipoprotein profile and in LMM and LHM.

C) Proportion of human (red) and murine (black) reads counts in the liver of humanized (LHM) or "murinized" (LMM) model.

D) Number of genes in all models of rhythmic gene expression (Figure 1B) in the liver of LMM and LHM (BICW > 0.3, log2 amplitude > 0.5).

E) Enrichment of up- and down-regulated genes in the liver of LMM and LHM for genes up- and down-regulated in the liver of mice KO for the negative (*Tsc1* KO) or positive (*Raptor* KO) regulators of mTOR (see methods).

F) Western blot analysis of Phospho-S6 Ribosomal Protein (Ser240/244) and total S6 Ribosomal Protein and non-linear cosinor fitting of P-RPS6 signal normalized by ponceau signal. Analysis of rhythmicity done with *dryR* (BICW = 0.572 for rhythmicity only in LMM).

G) Circulating murine growth hormone (GH) and Insulin-like growth factor-1 (IGF-1) in LMM and LHM. Data are expressed as mean +/- SEM (n=9-11 animals for each condition). *** P<0.0001.

H) Top. Female- (left) and male(right)-biased gene expression from control and humanized mouse livers at indicated Zeitgeber Time (color). Bottom. The predicted activity of sex-dependent (female (♀, left) and male (♂, right) target genes of STAT5 in the mouse liver. P values were determined by a two-way ANOVA (time, condition), P value for condition is reported (n = 12 mice per condition).

Fig. S2

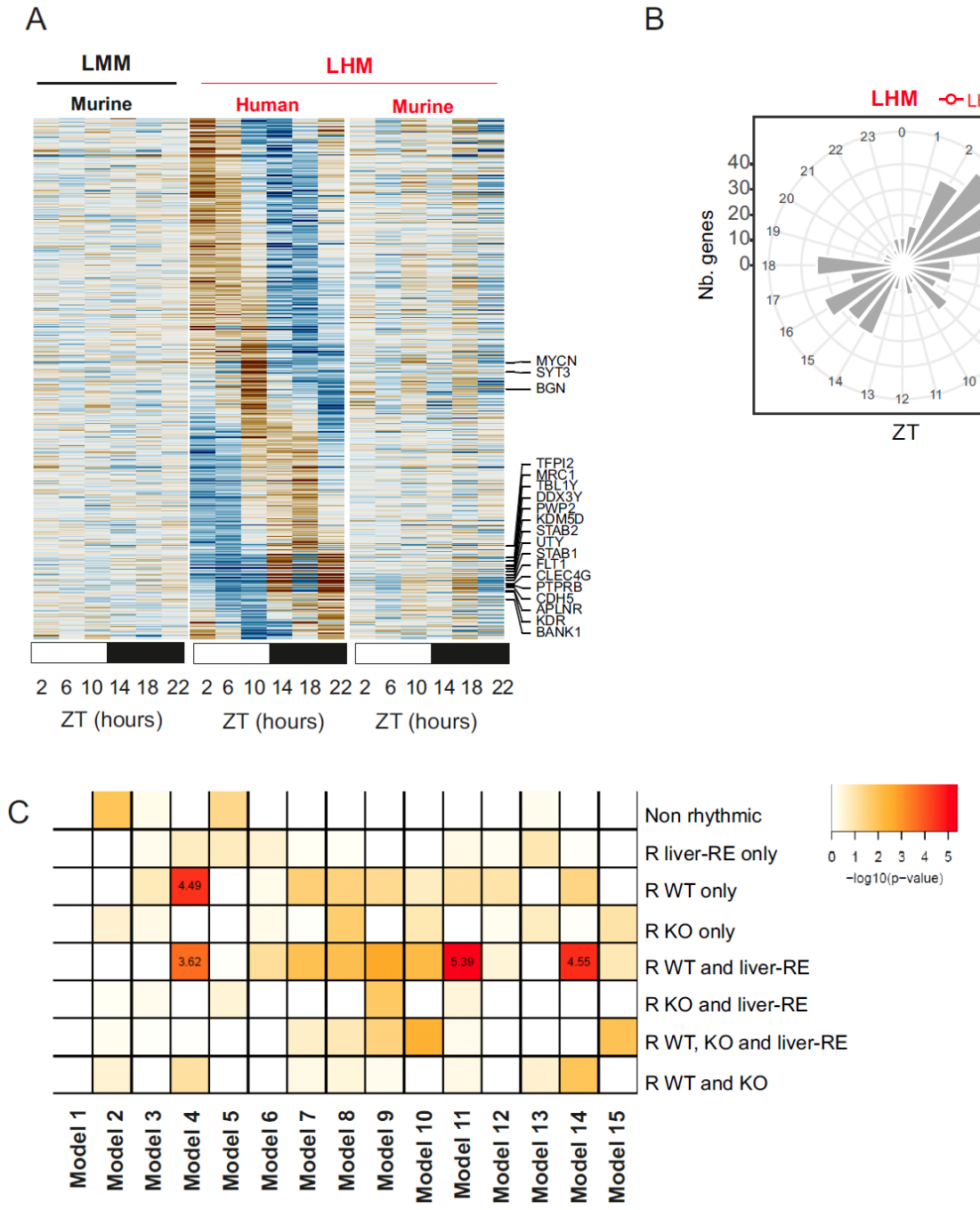

Fig.S2. Impact of the engrafted human hepatocytes on liver rhythmic gene expression

A, **B**) Heat maps (**A**) and radial plots of the distribution of the peak phase (**B**) of normalized rhythmic mRNA levels (BICW > 0.5, log2 amplitude > 0.5) in the liver of LMM (black) and LHM (red). Genes are assigned to model 2 in which only human genes are rhythmic in LHM animals while non-rhythmic in LMM.

C) Enrichment of the rhythmic genes (-log10 p-value, hypergeometric test, see method) in the liver of LMM and LHM ranked in the 15 models of rhythmicity for genes rhythmic in all combinations of WT,

Bmal1 KO (KO), and hepatocyte-specific *Bmal1* rescue in *Bmal1* KO animals (liver-RE). While genes directly regulated by BMAL1 (rhythmic in WT and liver-KO) are enriched in models 4 (rhythmic only in LMM), 11 (same rhythm in LMM and mouse and human transcripts in LMM), and 14 (rhythmic in all conditions but different phase in LMM), rhythmic genes dependent on systemic cues regulated by BMAL1 (rhythmic only in WT) are enriched only in model 4, showing that the rhythm of many of these genes depends on systemic signals regulated by the circadian clock in non-liver tissues.

Fig. S3

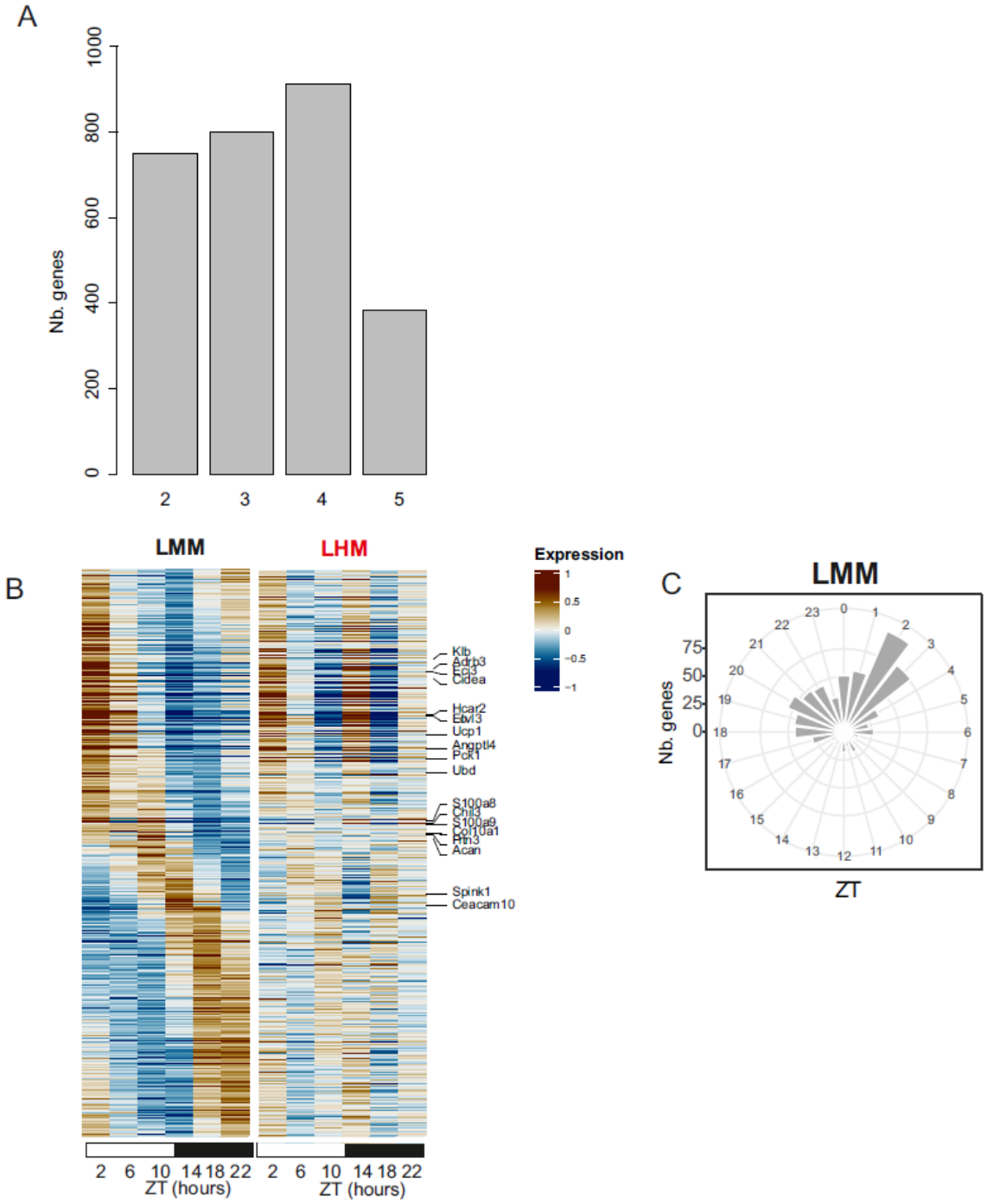

Fig.S3. The muscle circadian clock of liver humanized mice is phase advanced

A) Number of genes in all models of rhythmic gene expression (Figure 3A) in the muscle of LMM and LHM (BICW > 0.5, log2 amplitude > 0.5).

B, **C**) Heat maps (**B**) and radial plots of the distribution of the peak phase (**C**) of normalized rhythmic mRNA levels (BICW > 0.5, log2 amplitude > 0.5) in the muscle of LMM (black) and LHM (red). Genes are assigned to model 3 in which mRNA are only rhythmic in LMM.

Fig. S4

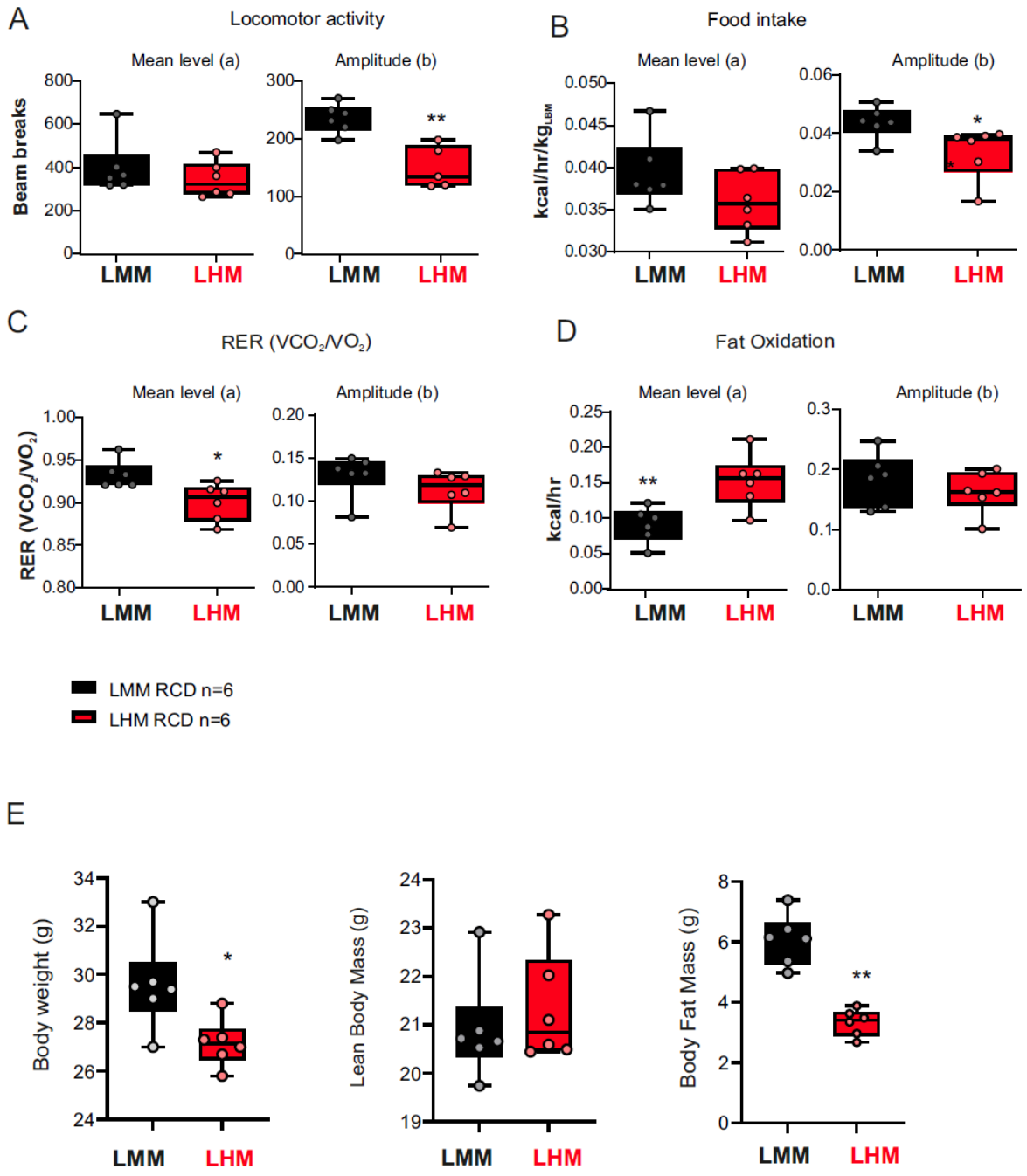

Fig.S4. Human hepatocytes advance the phase of circadian metabolism and behavior of liver humanized mice

A-D) Cosinor analysis of the rhythmic parameters mean level (a) and amplitude (b) for locomotor activity (**A**), food intake (**B**), RER (**C**), and fat oxidation (**D**). Data are expressed as mean +/- SEM (n=6 animals per condition). * P<0.05, ** P<0.01

E) Averaged values for body weight, lean body mass, and fat mass in LMM (black) and LHM (red) at the beginning of the experiment. Data are expressed as mean +/- SEM (n=6 per condition). P values were determined by a one-way ANOVA. * $P<0.05$, ** $P<0.01$.

Fig. S5

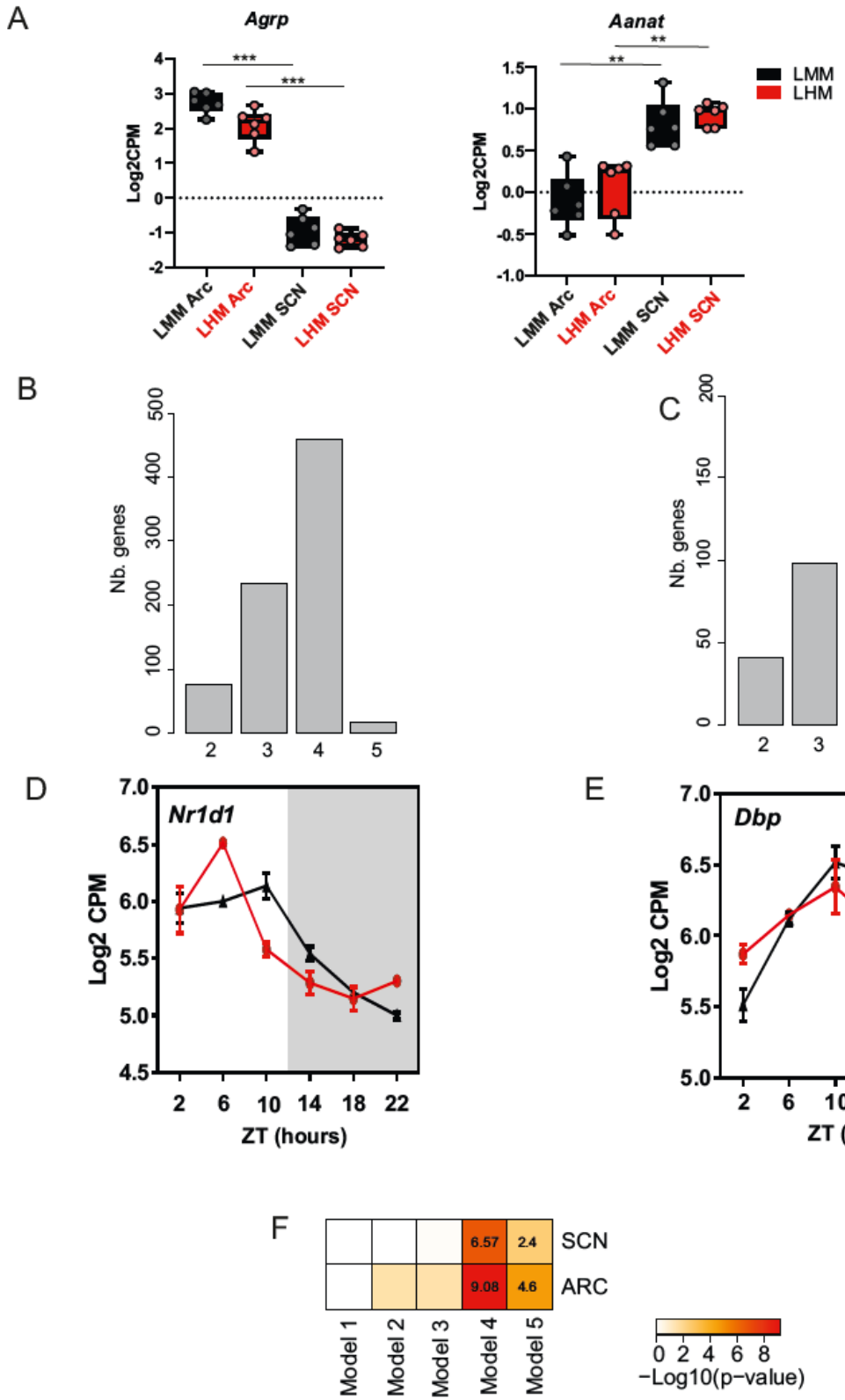

Fig.S5. Engrafted human hepatocytes impact rhythmic gene expression in the hypothalamus A) Expression level of the ARC-enriched *Agouti-related transcript* (*Agrp*) and the SCN-enriched

Aralkylamine N-Acetyltransferase (*Aanat*) in the dissected ARC and SCN of LMM (black) and LHM (red). **

B, **C**) Number of genes in all models of rhythmic gene expression (Figure 5A) in the SCN (**B**) and ARC (**C**) of LMM and LHM.

D, **E**) Rhythmic expression of the circadian clock regulated genes *Nr1d1* (D) and *Dbp* (E) in the SCN and ARC, respectively, of LMM and LHM.

F) Enrichment of the rhythmic genes in the SCN and ARC of LMM and LHM ranked in the 5 models of rhythmicity for genes bound by CLOCK in ChIP-Seq experiment (see Method).

Fig. S6

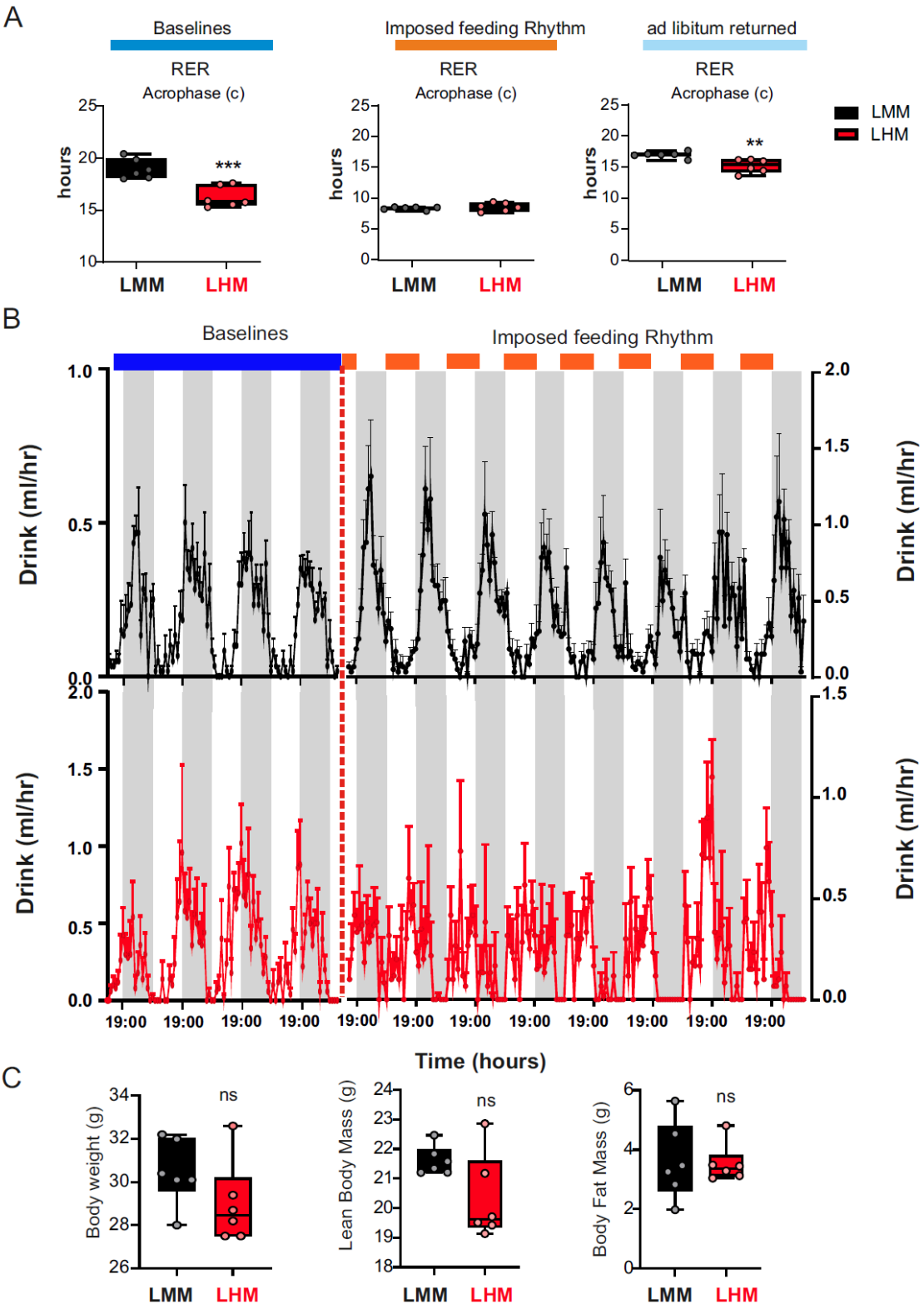

Fig.S6. Engraftment of human hepatocytes reveals the ability of hepatic signals to feedback on the central pacemaker

A) Cosinor analysis of the acrophase (c) for RER during baseline (left), imposed feeding during the light phase (middle), and after return to *ad libitum* feeding (right). Data are expressed as mean +/- SEM (n=6 per condition). ** P<0.01, *** P<0.0001.

B) Averaged values and kinetics of water intake in LMM mice (black upper panel) and LHM mice (red, lower panel) during baselines (blue, left Y axis) and imposed feeding rhythm (orange, right Y axis).

C) Averaged values for body weight, lean body mass, and fat mass in LMM (black) and LHM (red) at the beginning of the experiment. Data are expressed as mean +/- SEM (n=6 per condition). P values were determined by a one-way ANOVA.

Table S1. RNA-Seq analysis results of rhythmic gene expression in different tissues of LMM and LHM

Sheet 1. Detailed table legend. Sheet 2. Results of the rhythmicity analysis using multiple generalized linear regression and model selection in liver of LHM and LMM. Sheet 3. Results of the rhythmicity analysis using multiple generalized linear regression and model selection in skeletal muscle of LHM and LMM. Sheet 4. Results of the rhythmicity analysis using multiple generalized linear regression and model selection in the SCN of LHM and LMM. Sheet 5. Results of the rhythmicity analysis using multiple generalized linear regression and model selection in the ARC of LHM and LMM.

Table S2. GO terms associated with differentially rhythmic genes in the liver of LHM and LMM depending on the model of rhythmicity

Sheet 1. Detailed table legend. Sheet 2. Biological Process associated with differential rhythmic genes in liver for genes in Model 2. Sheet 3. Biological Process associated with differential rhythmic genes in liver for genes in Model 3. Sheet 4. Biological Process associated with differential rhythmic genes in liver for genes in Model 4. Sheet 5. Biological Process associated with differential rhythmic genes in liver for genes in Model 5. Sheet 6. Biological Process associated with differential rhythmic genes in liver for genes in Model 6. Sheet 7. Biological Process associated with differential rhythmic genes in liver for genes in Model 7. Sheet 8. Biological Process associated with differential rhythmic genes in liver for genes in Model 8. Sheet 9. Biological Process associated with differential rhythmic genes in liver for genes in Model 9. Sheet 10. Biological Process associated with differential rhythmic genes in liver for genes in Model 10. Sheet 11. Biological Process associated with differential rhythmic genes in liver for genes in Model 13. Sheet 12. Biological Process associated with differential rhythmic genes in liver for genes in Model 14. Sheet 13. Biological Process associated with differential rhythmic genes in liver for genes in Model 15.

Table S3. GO terms associated with differentially rhythmic genes in the skeletal muscle of LHM and LMM depending on the model of rhythmicity

Sheet 1. Detailed table legend. Sheet 2. Biological Process associated with differential rhythmic genes in skeletal muscle for genes in Model 2. Sheet 3. Biological Process associated with differential rhythmic genes in skeletal muscle for genes in Model 3. Sheet 4. Biological Process associated with differential rhythmic genes in skeletal muscle for genes in Model 4. Sheet 5. Biological Process associated with differential rhythmic genes in skeletal muscle for genes in Model 5.

Table S4. GO terms associated with differentially rhythmic genes in the SCN of LHM and LMM depending on the model of rhythmicity

Sheet 1. Detailed table legend. Sheet 2. Biological Process associated with differential rhythmic genes in the SCN for genes in Model 2. Sheet 3. Biological Process associated with differential rhythmic genes

in the SCN for genes in Model 3. Sheet 4. Biological Process associated with differential rhythmic genes in the SCN for genes in Model 4. Sheet 5. Biological Process associated with differential rhythmic genes in the SCN for genes in Model 5.

Table S5. GO terms associated with differentially rhythmic genes in the ARC of LHM and LMM depending on the model of rhythmicity

Sheet 1. Detailed table legend. Sheet 2. Molecular functions associated with differential rhythmic genes in the ARC for genes in Model 2. Sheet 3. Molecular functions associated with differential rhythmic genes in the ARC for genes in Model 3. Sheet 4. Molecular functions associated with differential rhythmic genes in the ARC for genes in Model 4.Table.S1. RNA-Seq analysis results of rhythmic gene expression in different tissues of LMM and LHM